Electron-phonon correlations inducing excitonic excitations in semimetal and semiconducting materials

Thi-Hong-Hai Do [1] and Van-Nham Phan [2,3,*]

[1]*Department of Physics, Hanoi University of Mining and Geology, Duc Thang, Bac Tu Liem, Hanoi, Vietnam*
[2]*Institute of Research and Development, Duy Tan University, 3 Quang Trung, Danang, Vietnam*
[3]*Faculty of Natural Sciences, Duy Tan University, 3 Quang Trung, Da Nang, Vietnam*

The influence of phonons on the low-energy excitonic excitations at zero temperature in the extended Falicov-Kimball model has been investigated. In the framework of the unrestricted Hartree-Fock approximation, a set of self-consistent equations for the excitonic condensate order parameter and a lattice distortion is derived when both electron-phonon coupling and electron-hole Coulomb interaction are treated on an equal footing. The low-energy excitation properties of the excitonic condensate are addressed in signatures of the optical conductivity and the dynamical excitonic susceptibility function. The real part of the optical conductivity is evaluated by the Kubo linear response theory and the imaginary part of the dynamical excitonic susceptibility is found by adapting the random phase approximation. In the semimetal state, one always finds a sharp peak in the optical conductivity spectrum indicating the stability of the excitonic condensation in the BCS type if the correlation between electrons and phonons becomes significant. In contrast, the peak is smeared out on the semiconducting side indicating the stability of the BEC-type excitonic condensate. In this semiconducting side, the sharp peak signature appears and the system turns to the BCS-type excitonic condensation state by increasing the electron-phonon correlations. In either the semimetal or the semiconducting normal state, increasing the electron-phonon correlations always reinforces a low-energy sharp peak in the dynamical excitonic susceptibility spectrum, indicating the existence of the tightly bound excitonic excitations before the condensation state. Specifically, on the semiconducting side, the "halo" phase with the preformed excitons exiting outside of the BEC-excitonic condensation state has been specified. The halo phase becomes more recognizable by raising the electron-phonon correlations.

I. INTRODUCTION

The Bose-Einstein condensation (BEC) state is one of the most interesting quantum phenomena attracting much interest both in science and in technology. The BEC state might be observed in a system of bosonic particles or quasiparticles with sufficiently large density once all these bosons condense spontaneously into a single coherent quantum state at a very low temperature. The exciton is one of the bosonic quasiparticles that might be formed in a small band-overlap semimetal or in a narrow band-gap semiconductor due to the Coulomb attraction between an electron in a conduction band and a hole in a valance band [1]. Once the temperature is sufficiently low, the excitons might condense into the BEC so-called excitonic insulator (EI) state that has been conceived more than 60 years ago [2–4]. Depending on either large or small Coulomb coupling, the excitons might condense like the Cooper pairs in the Bardeen-Cooper-Schrieffer (BCS) theory or like neutral atoms in the original BEC consideration [5,6].

As addressed above, the exciton is a bound state of an electron and hole mediated by the Coulomb interaction, thus to analyze the formalism of the excitonic condensation, it is naturally investigated in a purely electronic manner [2–8].

However, in some circumstances, phononic signatures also play important roles in reinforcing the stability of the excitonic condensation state [9–11]. Indeed, an experiment has revealed that an abrupt change of lattice displacement just heats up the excitonic condensate in the mixed valence compound $TmSe_{0.45}Te_{0.55}$ [12]. In transition-metal dichalcogenide $1T\text{-}TiSe_2$, one has specified a strong relation between the charge-density-wave and excitonic condensation state [13,14]. The lattice distortion is also believed as a crucial point pushing up the critical temperature of the excitonic condensation state to the record value up to $T_c = 326$ K in Ta_2NiSe_5 [11,15–17]. From several points of view, involving the phononic degree of freedom is crucially important to inspect the underlying physics of the excitonic condensation state in some semimetal/semiconductor materials. In our present work, the electron-hole system is described in the framework of the extended Falicov-Kimball model (EFKM) where the valance electrons are able to hop but the Coulomb interaction is localized. The phononic involvement is addressed by the electron-phonon interaction. Both the electronic and the phononic degrees of freedom are thus involved equally to address signatures of the excitonic instability in the systems.

Utilizing the EFKM with the electron-phonon interaction, the excitonic instability has been considered [14,18–20]. In these studies, the excitonic stability is specified by analyzing the excitonic condensate order parameter and only some static

---

*Corresponding author: phanvannham@duytan.edu.vn

signatures of the order state are addressed. In the meanwhile, in order to understand the nature of an ordered state, the fluctuations both inside and outside of the ordered state need to be cleared [11,16,21–25]. Indeed, by inspecting the dynamical excitonic susceptibility function, one has specified the fluctuations of a bound coherent state corresponding to the formation of the preformed excitons before the excitonic stability in the semiconductor, the so-called "halo" of the excitonic condensation state [21]. The halo phase has been experimentally observed in the semiconductor compound TmSe$_{0.45}$Te$_{0.55}$ [12,26]. By analyzing the optical conductivity spectra one also revealed the anomalous appearance of the excitons even before the excitonic condensation in metallic Ta$_2$NiSe$_5$ [22,23]. In our present work, the anomalies of the preformed excitons existing outside of the condensation state would be considered by analyzing the optical conductivity and dynamical excitonic susceptibility function. Without electron-phonon coupling, these dynamical quantities of the EFKM have been addressed [27]. In that study, the resonance of the coherent excitonic state before the stability of the excitonic condensate in the halo phase has been specified on the semiconductor side. In the presence of phonons, our present study would describe the nature of the resonance coherent state on the impact of the electron-phonon correlations. Our results reveal that the halo phase can be found for large Coulomb interaction. Increasing the electron-phonon correlations leads to reinforcing the resonance of the coherent state that appears even on the semimetal side.

In the present work, the EFKM with electron-phonon coupling is considered in the framework of the unrestricted Hartree-Fock (UHF) approximation. By neglecting all fluctuations raised due to many-particle correlations, one can simply derive a single-particle effective model, thus a set of self-consistent equations determining the excitonic condensate order parameters or quasi-particle energies is easily delivered. With the results of the effective Hamiltonian, one can explicitly evaluate the optical conductivity in the features of Kubo linear response theory and the dynamical excitonic susceptibility function in the random phase approximation. Once a solution of the set of self-consistent equations is numerically achieved, signatures of the optical conductivity or dynamical excitonic susceptibility spectrum can be observed. That helps us explicitly analyze the dynamical properties of the excitons around the critical points under the influence of phonons and also other parameters. We agree that the UHF approximation generally is insufficient in considering the correlated electron systems. However, in some specific conditions, the UHF approach is still applicable even for large interacting cases such as in the cases of very high and very low temperature limitations [28–31]. In the situation of very low temperature, one has pointed out that the UHF approximation is equivalent to the dynamical mean-field theory—one of the best theoretical approaches successfully applied to the strongly correlated electron systems [29,32], or to the unbiased constrained path Monte Carlo simulation [33,34]. In our investigation we consider the system in the ground state, i.e., at zero temperature. The results of the phase diagram and optical conductivity in our work are thus reliable [22,35].

This paper is organized as follows. In the next section, Sec. II, the Hamiltonian of the EFKM involving the electron-phonon correlations is addressed. In Sec. III, the analytical calculation evaluating the effective Hamiltonian in the UHF approximation is derived; it then is applied to find the analytical expressions of the optical conductivity and the excitonic susceptibility function. The numerical results and discussion can be found in Sec. IV. Finally, Sec. V summarizes our work.

II. EXTENDED FALICOV-KIMBALL MODEL WITH ELECTRON-PHONON COUPLING

In order to address the influence of phonons to the excitonic excitation state we use here the spinless extended EFKM involving the electron-phonon correlations. Both the electron-hole Coulomb attraction and electron-phonon coupling thus are treated on an equal footing. In the momentum space, the EFKM with the electron-phonon coupling can be written as follows:

$$
\begin{aligned}
\mathcal{H} =& \sum_{\mathbf{k}} \left(\varepsilon^a_{\mathbf{k}} a^\dagger_{\mathbf{k}} a_{\mathbf{k}} + \varepsilon^b_{\mathbf{k}} b^\dagger_{\mathbf{k}} b_{\mathbf{k}} + \omega_0 p^\dagger_{\mathbf{k}} p_{\mathbf{k}} \right) \\
&+ \frac{U}{N} \sum_{\mathbf{kk'q}} b^\dagger_{\mathbf{k}+q} b_{\mathbf{k'}} a^\dagger_{\mathbf{k'}-q} a_{\mathbf{k}} \\
&+ \frac{g}{\sqrt{N}} \sum_{\mathbf{kq}} [b^\dagger_{\mathbf{k}+\mathbf{q}} a_{\mathbf{k}} (p^\dagger_{-\mathbf{q}} + p_{\mathbf{q}}) + \text{H.c.}],
\end{aligned}
\tag{1}
$$

where $a^\dagger_{\mathbf{k}}$ ($a_{\mathbf{k}}$), $b^\dagger_{\mathbf{k}}$ ($b_{\mathbf{k}}$), and $p^\dagger_{\mathbf{k}}$ ($p_{\mathbf{k}}$) are the creation (annihilation) operators of the conduction a, valance b electrons and phonons at momentum $\mathbf{k}$, respectively. The first line in Hamiltonian (1) expresses the kinetic energy of the electron-hole-phonon system where $\varepsilon^{a(b)}_{\mathbf{k}}$ and ω_0 are, respectively, the electrononic dispersion of a (b) electrons and of phononic dispersion. To simplify our further calculation we use the dispersionless energy of the phonon described by the Einstein frequency ω_0 and the electronic dispersion energy of the electrons, written in the tight-binding approximation, that read

$$
\varepsilon^{a(b)}_{\mathbf{k}} = \varepsilon^{a(b)} - t^{a(b)} \gamma_{\mathbf{k}} - \mu.
\tag{2}
$$

Here $\varepsilon^{a(b)}$ and $t^{a(b)}$ are, respectively, the on-site energy and hopping integral of the $a(b)$ electrons with $\gamma_{\mathbf{k}} = 2(\cos k_x + \cos k_y)$ written in a two-dimensional (2D) hypercubic lattice. μ here is the chemical potential. The difference between the on-site energies $\Delta \varepsilon = \varepsilon^a - \varepsilon^b$ gives us a separation between the conduction and valance electronic bands. In the case with $\Delta \varepsilon > 0$ one finds a semiconducting situation and with $\Delta \varepsilon < 0$ one finds a semimetal state. Without losing the generality, $t^a = 1$ is chosen as the unit of energy and $|t^b| < 1$ is often fixed to address the heavier dispersive electrons in the valance band. The Hamiltonian in Eq. (1) has been also written in the general units with $\hbar = c = k_B = 1$ [36].

In the Hamiltonian (1), the second and the last lines express the interband electron-hole Coulomb interaction and the electron-phonon coupling in the system, respectively, with N being a number of lattice sites. Both the Coulomb interaction U and the electron-phonon coupling g here are assumed to be localized. The assumption is applicable to consider the excitonic condensation state in almost semimetal/semiconducting materials with the conduction and the valence electrons coupling together on the same site [6,22,37]. In Eq. (1) we also

omit all other Coulomb interactions such as between *a-a* or *b-b* electrons to simplify our further calculation. The interactions mainly shift the on-site energy levels of the *a* or *b* electrons only and they do not strongly affect the electron-hole or electron-phonon correlations in the excitonic excitation signatures in the system.

III. THEORETICAL CALCULATION

A. Unrestricted Hartree-Fock aproximation

The model written in Eq. (1) is the many-particle correlation quantum Hamiltonian. There is thus no way to solve it exactly. Generally, one has to try simplifying the many-body features to a single-particle Hamiltonian by applying some approximations. In this study, we use the UHF approximation to solve the Hamiltonian written in Eq. (1). Within this approximation, all fluctuation parts are possibly ignored and one might find an effective single-particle Hamiltonian, that reads

$$\mathcal{H}_{\text{UHF}} = \sum_{\mathbf{k}} \left(\bar{\varepsilon}_{\mathbf{k}}^a a_{\mathbf{k}}^\dagger a_{\mathbf{k}} + \bar{\varepsilon}_{\mathbf{k}}^b b_{\mathbf{k}}^\dagger b_{\mathbf{k}} + \omega_0 p_{\mathbf{k}}^\dagger p_{\mathbf{k}} \right)$$
$$+ \delta \sum_{\mathbf{k}} (b_{\mathbf{k}}^\dagger a_{\mathbf{k}} + \text{H.c.}) + \sqrt{N} h(p_{-\mathbf{q}}^\dagger + p_{\mathbf{q}}) \delta_{\mathbf{q},\mathbf{0}}. \quad (3)$$

Here we have assumed that the system stabilizes in the excitonic condensation state, specified by the presence of spontaneous fields risen due to the stability of the electron-hole bound coherent states. We have also supposed the predominance of zero-momentum excitons, i.e., with $\mathbf{q} = \mathbf{0}$, that have been specified condensing in a single coherent state in the case of the typical mixed-valance compound Ta$_2$NiSe$_5$ [11,16,17]. The spontaneous fields described in the second line of the effective Hamiltonian in Eq. (3) thus read

$$h = \frac{g}{N} \sum_{\mathbf{k}} \langle b_{\mathbf{k}}^\dagger a_{\mathbf{k}} + a_{\mathbf{k}}^\dagger b_{\mathbf{k}} \rangle, \quad (4)$$

$$\delta = \frac{g}{\sqrt{N}} \langle p_{-\mathbf{q}}^\dagger + p_{\mathbf{q}} \rangle \delta_{\mathbf{q},\mathbf{0}} - \frac{U}{N} \sum_{\mathbf{k}} \langle b_{\mathbf{k}}^\dagger a_{\mathbf{k}} \rangle. \quad (5)$$

In Eqs. (4) and (5), both h and δ contain a term representing a hybridization between the *a* and *b* electrons, $\langle b_{\mathbf{k}}^\dagger a_{\mathbf{k}} \rangle$, corresponding to a formation of excitons and their condensation state. They thus play the role of the excitonic condensate order parameters.

In the UHF approximation, the electronic excitation energies have been shifted by the Coulomb interaction contribution given by

$$\bar{\varepsilon}_{\mathbf{k}}^{a(b)} = \varepsilon_{\mathbf{k}}^{a(b)} + U n^{b(a)}, \quad (6)$$

where $n^a = \sum_{\mathbf{k}} \langle a_{\mathbf{k}}^\dagger a_{\mathbf{k}} \rangle / N$ and $n^b = \sum_{\mathbf{k}} \langle b_{\mathbf{k}}^\dagger b_{\mathbf{k}} \rangle / N$ respectively are the density of *a* and *b* electrons. To find a close set of self-consistent equations, in the next step, we diagonalize the effective Hamiltonian in Eq. (3). In order to diagonalize the Hamiltonian we divide Eq. (3) into two parts: a so-called electronic part and a phononic one. The former part reads

$$\mathcal{H}_{\text{UHF}}^e = \sum_{\mathbf{k}} \left(\bar{\varepsilon}_{\mathbf{k}}^a a_{\mathbf{k}}^\dagger a_{\mathbf{k}} + \bar{\varepsilon}_{\mathbf{k}}^b b_{\mathbf{k}}^\dagger b_{\mathbf{k}} \right) + \delta \sum_{\mathbf{k}} (b_{\mathbf{k}}^\dagger a_{\mathbf{k}} + \text{H.c.}), \quad (7)$$

that can be diagonalized by using a Bogoliubov transformation with new fermionic operators

$$c_{\mathbf{k}}^\dagger = \xi_{\mathbf{k}} b_{\mathbf{k}}^\dagger + \eta_{\mathbf{k}} a_{\mathbf{k}}^\dagger, \quad (8)$$

$$f_{\mathbf{k}}^\dagger = -\eta_{\mathbf{k}} b_{\mathbf{k}}^\dagger + \xi_{\mathbf{k}} a_{\mathbf{k}}^\dagger, \quad (9)$$

where $\xi_{\mathbf{k}}$ and $\eta_{\mathbf{k}}$ are chosen such that $\xi_{\mathbf{k}}^2 + \eta_{\mathbf{k}}^2 = 1$. Then

$$\xi_{\mathbf{k}}^2 = \frac{1}{2} \left[1 + \text{sgn}\left(\bar{\varepsilon}_{\mathbf{k}}^a - \bar{\varepsilon}_{\mathbf{k}}^b \right) \frac{\bar{\varepsilon}_{\mathbf{k}}^a - \bar{\varepsilon}_{\mathbf{k}}^b}{\Gamma_{\mathbf{k}}} \right], \quad (10)$$

$$\eta_{\mathbf{k}}^2 = \frac{1}{2} \left[1 - \text{sgn}\left(\bar{\varepsilon}_{\mathbf{k}}^a - \bar{\varepsilon}_{\mathbf{k}}^b \right) \frac{\bar{\varepsilon}_{\mathbf{k}}^a - \bar{\varepsilon}_{\mathbf{k}}^b}{\Gamma_{\mathbf{k}}} \right], \quad (11)$$

with

$$\Gamma_{\mathbf{k}} = \sqrt{\left(\bar{\varepsilon}_{\mathbf{k}}^b - \bar{\varepsilon}_{\mathbf{k}}^a \right)^2 + 4|\delta|^2}. \quad (12)$$

The Hamiltonian in Eq. (7) thus can be completely diagonalized; it reads

$$\mathcal{H}_{\text{dia}}^e = \sum_{\mathbf{k}} \left(E_{\mathbf{k}}^c c_{\mathbf{k}}^\dagger c_{\mathbf{k}} + E_{\mathbf{k}}^f f_{\mathbf{k}}^\dagger f_{\mathbf{k}} \right), \quad (13)$$

where the quasiparticle energies are given by

$$E_{\mathbf{k}}^{c/f} = \frac{\bar{\varepsilon}_{\mathbf{k}}^a + \bar{\varepsilon}_{\mathbf{k}}^b}{2} \mp \frac{\text{sgn}\left(\bar{\varepsilon}_{\mathbf{k}}^a - \bar{\varepsilon}_{\mathbf{k}}^b \right)}{2} \Gamma_{\mathbf{k}}. \quad (14)$$

From Eq. (19), the expectation values could be evaluated and we obtain

$$\langle n_{\mathbf{k}}^b \rangle = \langle b_{\mathbf{k}}^\dagger b_{\mathbf{k}} \rangle = \xi_{\mathbf{k}}^2 f\left(E_{\mathbf{k}}^c \right) + \eta_{\mathbf{k}}^2 f\left(E_{\mathbf{k}}^f \right),$$
$$\langle n_{\mathbf{k}}^a \rangle = \langle a_{\mathbf{k}}^\dagger a_{\mathbf{k}} \rangle = \eta_{\mathbf{k}}^2 f\left(E_{\mathbf{k}}^c \right) + \xi_{\mathbf{k}}^2 f\left(E_{\mathbf{k}}^f \right),$$
$$\langle d_{\mathbf{k}} \rangle = \langle b_{\mathbf{k}}^\dagger a_{\mathbf{k}} \rangle = -\left[f\left(E_{\mathbf{k}}^c \right) - f\left(E_{\mathbf{k}}^f \right) \right] \text{sgn}\left(\bar{\varepsilon}_{\mathbf{k}}^a - \bar{\varepsilon}_{\mathbf{k}}^b \right) \frac{\delta}{\Gamma_{\mathbf{k}}}, \quad (15)$$

where $f(\epsilon) = 1/(1 + e^{\beta \epsilon})$ is the Fermi-Dirac distribution function, with $\beta = 1/T$ and T is the temperature.

The phononic part of the Hamiltonian in Eq. (3),

$$\mathcal{H}_{\text{UHF}}^{\text{ph}} = \sum_{\mathbf{k}} \omega_0 p_{\mathbf{k}}^\dagger p_{\mathbf{k}} + \sqrt{N} h(p_{-\mathbf{q}}^\dagger + p_{\mathbf{q}}) \delta_{\mathbf{q},\mathbf{0}}, \quad (16)$$

that can be diagonalized by defining a new phononic operator

$$P_{\mathbf{k}}^\dagger = p_{\mathbf{k}}^\dagger + \sqrt{N} \frac{h}{\omega_0} \delta_{\mathbf{k},\mathbf{0}}, \quad (17)$$

and its diagonalized form results in

$$\mathcal{H}_{\text{dia}}^{\text{ph}} = \sum_{\mathbf{k}} \omega_0 P_{\mathbf{k}}^\dagger P_{\mathbf{k}}. \quad (18)$$

Here one can find from Eq. (17) that

$$\langle p_{-\mathbf{q}}^\dagger + p_{\mathbf{q}} \rangle = -2 \frac{\sqrt{N} h}{\omega_0} \delta_{\mathbf{q},\mathbf{0}}, \quad (19)$$

where $\delta_{\mathbf{q},\mathbf{0}}$ indicates that there are only zero-momentum phonons mediating the excitonic bound state in the system. Note that the phonon here is considered in the optical mode only, described in the Einstein model. The phonon scattering still thus happens even at zero momentum $\mathbf{q} = \mathbf{0}$.

From Eqs. (4), (5), (15), and (19) one finds a set of self-consistent equations determining the excitonic condensate order parameters h or δ and evaluating the quasiparticle excitation energies both inside and outside of the excitonic

condensation state. The quantities help us probe signatures of the optical conductivity and excitonic dynamical susceptibility spectra.

B. The optical conductivity

One of the most essential steps towards understanding the critical problem of excitonic phases is probing the dynamical signatures of the excitonic condensation state. In our present work, optical characterization describing the critical problem is examined in a sense of optical conductivity. Utilizing the Kubo formula of the linear response theory [38], the real part of the optical conductivity depending on frequency could be given as the real part of the two-particle retarded correlation function

$$\sigma(\omega) = \text{Re} \frac{i}{\omega N^2} \sum_{\mathbf{kk'}} \langle\langle \mathbf{j}^\dagger(\mathbf{k}) | \mathbf{j}(\mathbf{k'}) \rangle\rangle_\omega, \quad (20)$$

where $\mathbf{j}(\mathbf{k})$ is the momentum dependence of the current operator, defined by

$$\mathbf{j}(\mathbf{k}) = v_{\mathbf{k}}^a a_{\mathbf{k}}^\dagger a_{\mathbf{k}} + v_{\mathbf{k}}^b b_{\mathbf{k}}^\dagger b_{\mathbf{k}}, \quad (21)$$

where $v_{\mathbf{k}}^{a(b)} = \nabla \varepsilon_{\mathbf{k}}^{a(b)}$ is the velocity of the a (b) electron. Using the Bogoliubov transformation in Eqs. (8) and (9), the current operators can be represented in the new quasiparticle fermionic operators $c_{\mathbf{k}}^\dagger$ ($c_{\mathbf{k}}$) and $f_{\mathbf{k}}^\dagger$ ($f_{\mathbf{k}}$). With the help of the diagonal Hamiltonian $\mathcal{H}_{\text{dia}}$ in Eq. (19), one easily evaluates an expression for the real part of the optical conductivity

$$\sigma(\omega) = \frac{\pi e^2}{\omega N} \sum_{\mathbf{k}} \eta_{\mathbf{k}}^2 \xi_{\mathbf{k}}^2 \left(v_{\mathbf{k}}^a - v_{\mathbf{k}}^b\right)^2 \left[f\left(E_{\mathbf{k}}^c\right) - f\left(E_{\mathbf{k}}^f\right)\right]$$
$$\times \left[\delta\left(\omega + E_{\mathbf{k}}^c - E_{\mathbf{k}}^f\right) - \delta\left(\omega - E_{\mathbf{k}}^c + E_{\mathbf{k}}^f\right)\right]. \quad (22)$$

Here the coefficients $\eta_{\mathbf{k}}$ and $\xi_{\mathbf{k}}$ have been defined in Eqs. (10) and (11) and the quasiparticle excitation energies $E_{\mathbf{k}}^{c/f}$ are given in Eq. (14). All these quantities can be evaluated by solving the self-consistent equations found in the previous section. The frequency dependence of the optical conductivity then could be probed.

C. The excitonic susceptibility function

Another quantity essentially to probe the dynamical excitations of the excitonic condensation state is the dynamical excitonic susceptibility function. At a given momentum $\mathbf{q}$, the dynamical excitonic susceptibility function can be written as

$$\chi(\mathbf{q}, \omega) = -\langle\langle X_{\mathbf{q}} | X_{\mathbf{q}}^\dagger \rangle\rangle_\omega, \quad (23)$$

where an operator $X_{\mathbf{q}}^\dagger = (1/\sqrt{N}) \sum_{\mathbf{k}} a_{\mathbf{k}+\mathbf{q}}^\dagger b_{\mathbf{k}}$ plays the role of the exciton creation operator. Unlike the optical conductivity in the previous section, evaluating the excitonic dynamical susceptibility in Eq. (23) appears the higher-order Green's functions which need to be truncated. Using the random phase approximation, one might find

$$\sum_{\mathbf{k''q_1}} \langle\langle a_{\mathbf{k}}^\dagger b_{\mathbf{k''}} a_{\mathbf{k''}-\mathbf{q_1}}^\dagger a_{\mathbf{k}+\mathbf{q}-\mathbf{q_1}} | b_{\mathbf{k'}+\mathbf{q}}^\dagger a_{\mathbf{k'}} \rangle\rangle_\omega$$
$$\approx \sum_{\mathbf{q_1}} \langle n_{\mathbf{k}+\mathbf{q}-\mathbf{q_1}}^a \rangle \langle\langle a_{\mathbf{k}}^\dagger b_{\mathbf{k}+\mathbf{q}} | b_{\mathbf{k'}+\mathbf{q}}^\dagger a_{\mathbf{k'}} \rangle\rangle_\omega$$
$$- \sum_{\mathbf{k_2}} \langle n_{\mathbf{k}}^a \rangle \langle\langle a_{\mathbf{k_2}}^\dagger b_{\mathbf{k_2}+\mathbf{q}} | b_{\mathbf{k'}+\mathbf{q}}^\dagger a_{\mathbf{k'}} \rangle\rangle_\omega, \quad (24)$$

and

$$\sum_{\mathbf{k''q_1}} \langle\langle b_{\mathbf{k}+\mathbf{q_1}}^\dagger b_{\mathbf{k''}} a_{\mathbf{k''}-\mathbf{q_1}}^\dagger b_{\mathbf{k}+\mathbf{q}} | b_{\mathbf{k'}+\mathbf{q}}^\dagger a_{\mathbf{k'}} \rangle\rangle_\omega$$
$$\approx \sum_{\mathbf{q_1}} \langle n_{\mathbf{k}+\mathbf{q_1}}^b \rangle \langle\langle a_{\mathbf{k}}^\dagger b_{\mathbf{k}+\mathbf{q}} | b_{\mathbf{k'}+\mathbf{q}}^\dagger a_{\mathbf{k'}} \rangle\rangle_\omega$$
$$- \sum_{\mathbf{k_2}} \langle n_{\mathbf{k}+\mathbf{q}}^b \rangle \langle\langle a_{\mathbf{k_2}}^\dagger b_{\mathbf{k_2}+\mathbf{q}} | b_{\mathbf{k'}+\mathbf{q}}^\dagger a_{\mathbf{k'}} \rangle\rangle_\omega, \quad (25)$$

and similarly, we get

$$\sum_{\mathbf{q_1}} \langle\langle a_{\mathbf{k}}^\dagger a_{\mathbf{k}+\mathbf{q}-\mathbf{q_1}} (p_{-\mathbf{q_1}}^\dagger + p_{\mathbf{q_1}}) | b_{\mathbf{k'}+\mathbf{q}}^\dagger a_{\mathbf{k'}} \rangle\rangle_\omega$$
$$\approx \langle n_{\mathbf{k}}^a \rangle \langle\langle (p_{-\mathbf{q}}^\dagger + p_{\mathbf{q}}) | b_{\mathbf{k'}+\mathbf{q}}^\dagger a_{\mathbf{k'}} \rangle\rangle_\omega \quad (26)$$

and

$$\sum_{\mathbf{q_1}} \langle\langle b_{\mathbf{k}+\mathbf{q_1}}^\dagger b_{\mathbf{k}+\mathbf{q}} (p_{-\mathbf{q_1}}^\dagger + p_{\mathbf{q_1}}) | b_{\mathbf{k'}+\mathbf{q}}^\dagger a_{\mathbf{k'}} \rangle\rangle_\omega$$
$$\approx \langle n_{\mathbf{k}+\mathbf{q}}^b \rangle \langle\langle (p_{-\mathbf{q}}^\dagger + p_{\mathbf{q}}) | b_{\mathbf{k'}+\mathbf{q}}^\dagger a_{\mathbf{k'}} \rangle\rangle_\omega. \quad (27)$$

Finally, we derive the excitonic susceptibility function for the system as follows:

$$\chi(\mathbf{q}, \omega) = \frac{-\chi^0(\mathbf{q}, \omega)}{1 + (U - g\Lambda_{\mathbf{q}}) \chi^0(\mathbf{q}, \omega)}, \quad (28)$$

where

$$\chi^0(\mathbf{q}, \omega) = \frac{1}{N} \sum_{\mathbf{k}} \frac{\langle n_{\mathbf{k}}^a \rangle - \langle n_{\mathbf{k}+\mathbf{q}}^b \rangle}{\omega + i0^+ - \bar{\varepsilon}_{\mathbf{k}+\mathbf{q}}^b + \bar{\varepsilon}_{\mathbf{k}}^a} \quad (29)$$

acts as the bare excitonic susceptibility function, and

$$\Lambda_{\mathbf{q}} = \frac{2g\omega_0}{(\omega + i0^+)^2 - \omega_0^2 - \dfrac{2g^2\omega_0 \chi^{0b}(\mathbf{q}, \omega)}{1 + U\chi^{0b}(\mathbf{q}, \omega)}}, \quad (30)$$

with

$$\chi^{0b}(\mathbf{q}, \omega) = \frac{1}{N} \sum_{\mathbf{k}} \frac{\langle n_{\mathbf{k}-\mathbf{q}}^b \rangle - \langle n_{\mathbf{k}}^a \rangle}{\omega + i0^+ - \bar{\varepsilon}_{\mathbf{k}}^a + \bar{\varepsilon}_{\mathbf{k}-\mathbf{q}}^b}. \quad (31)$$

Here $\bar{\varepsilon}_{\mathbf{k}}^{a,b}$ are given in Eq. (6). Note here that the dynamical excitonic susceptibility function is considered out of the excitonic condensation state, the excitonic order parameter is completely zero, and $\langle n_{\mathbf{k}}^{a(b)} \rangle = f(\bar{\varepsilon}_{\mathbf{k}}^{a(b)})$. In this sense, the dynamical excitonic susceptibility can be simply evaluated.

IV. NUMERICAL RESULTS AND DISCUSSION

The main focus of this work is analyzing the effects of the phonon on the dynamical excitations of the excitonic condensation phase in semiconductor/superconductor (SM/SC) materials. In this section, we therefore present numerical results showing the dynamical excitonic susceptibility function and the optical conductivity. Considering a 2D system with $N = 800 \times 800$ lattice sites at zero temperature, for a given set of the model parameters, one might find a solution of the self-consistent equations in Eqs. (4), (5), (15), and (19). The optical conductivity $\sigma(\omega)$ and the dynamical excitonic susceptibility function $\chi(\mathbf{q}, \omega)$ then can be evaluated following
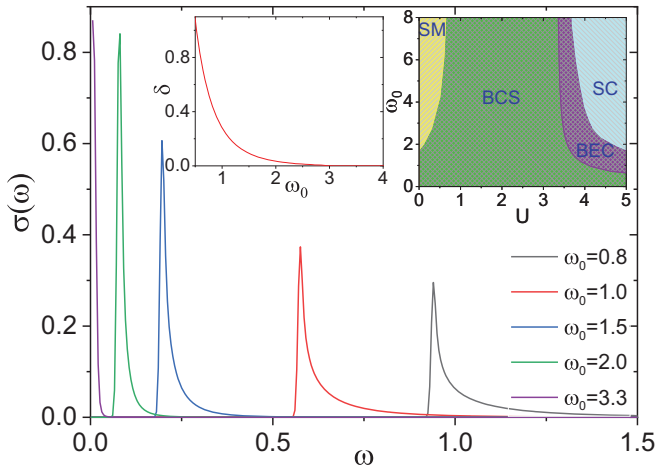
FIG. 1. The optical conductivity $\sigma(\omega)$ for different phonon frequencies ω_0 at $U = 0.4$ and $g = 0.6$. The left inset shows the excitonic condensate order parameter δ depending on ω_0. The right inset displays the ground-state phase diagram of the excitonic condensation state in the (U, ω_0) plane.

FIG. 2. The optical conductivity $\sigma(\omega)$ for different phonon frequencies ω_0 at $U = 4$ and $g = 0.6$. The left inset shows the excitonic condensate order parameter δ depending on phonon frequency ω_0. The right inset displays $\sigma(\omega)$ for $\omega_0 = 4$.

Eqs. (22) and (28), respectively. In the numerical calculation, we set $t^a = 1$ as the unit of energy and the results are fixed for $\varepsilon^a - \varepsilon^b = -2.0$. We also choose $t^b = -0.3 < 0$ characterizing the direct band gap as in the case of Ta$_2$NiSe$_5$ in which the excitonic condensation is driven by the strong electron-phonon coupling [11,15–17]. The chemical potential μ in Eq. (2) is adjusted to fix the total electronic number $n = n^a + n^b$. In the present study, we use $n = 1$ to ensure the half-filled band case.

We first discuss the phonon effects in the optical signatures of the excitonic condensate state by analyzing the influence of the phonon frequency on the optical conductivity spectrum. The optical conductivity might give us valuable information about the quasiparticle properties as well as the formation of excitonic states in the system. Figure 1 displays the optical conductivity $\sigma(\omega)$ for some values of the phonon frequency ω_0 for weak Coulomb interaction, $U = 0.4$ for instance, at the sufficiently large electron-phonon coupling $g = 0.6$. Note here that, for a weak Coulomb interaction, the system settles in the semimetal state and if the electron-phonon correlations are sufficiently large (indicated by small phonon energy and large electron-phonon coupling), the ground state of the system might stabilize in the excitonic condensate in BCS type (see the right inset). Indeed, for a given large electron-phonon coupling, e.g., $g = 0.6$, by lowering the phonon energy the excitonic condensate order parameter rapidly increases particularly in the adiabatic regime ($\omega_0 < t^a$) as shown in the left inset. The optical conductivity spectra in the main figure also address the dynamical signatures of the excitonic condensation state. Indeed, once the phonon energy is small the optical conductivity is completely zero as long as the frequency of the pulse light $\omega < 2\delta$. At $\omega = 2\delta$, the optical conductivity gets a sharp peak and then rapidly decreases as increasing ω as the optical conductivity of the normal metal. The appearance of the sharp peak in the optical conductivity spectrum at the frequency $\omega = 2\delta$ can be explained by the strong hybridization of the electrons and holes forming
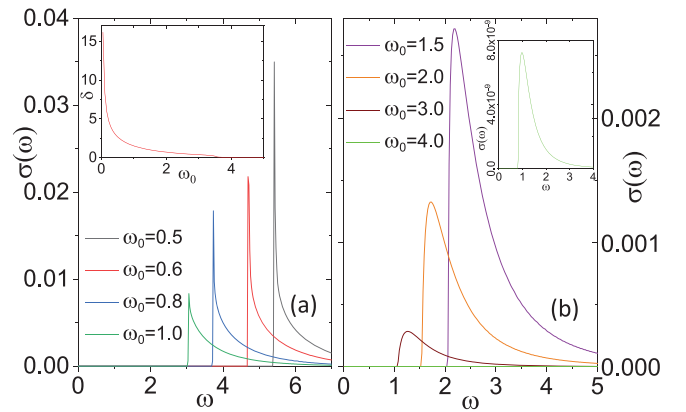
the excitonic bound state. This hybridization also causes the energy gap at the Fermi level in the quasiparticle energies. At low phonon frequency, the dynamics of the phonons is comparable to that of the electrons; the excitonic condensation state might be reinforced with the assistance of the electron-phonon correlations. That is illustrated by the appearance of a large frequency peak in the optical conductivity spectrum. Increasing the phonon frequency, the phononic level leaves far from the Fermi level and the phonon influence on the electron-hole pair correlations thus is depressed. The peak appearing in the optical conductivity spectrum thus moves to the lower frequency corresponding to a decrease of the excitonic condensate order parameter. Effects of the phonon oscillations on the excitonic condensation have been demonstrated by experimental observations in Ta$_2$NiSe$_5$ where the phase structure of the system changes from orthorhombic to monoclinic driven by the soft optical phonon modes [39,40]. At the phonon frequency, $\omega_0 > 3.3$, the sharp peak disappears and the optical conductivity characterizes the Drude form of the normal metallic state (see the purple line in Fig. 1).

In the case of sufficiently large Coulomb interaction, the large Hartree shift might open a band gap and the system settles in the semiconducting state. Due to the electron-phonon correlations, electron-hole pairs might be formed and condensed either in the BCS type or in the BEC type depending on the phonon frequency (see the right inset in Fig. 1) [41]. Note here that the boundary of the excitonic condensate is specified by detecting the divergence of the static excitonic susceptibility function $\chi^s = \chi(\mathbf{0}, \omega \to 0)$, where $\chi(\mathbf{q}, \omega)$ is defined in Eq. (28). The BCS and BEC types of the condensation are specified by the behavior of the momentum dependence of the excitonic condensate order parameter $d_{\mathbf{k}}$ in Eqs. (15). Indeed, on the BCS side, only electrons and holes settling near the Fermi surface might build up the electron-hole pairs and then condense. In this case, the electron-hole pair distribution $d_{\mathbf{k}}$ peaks at a finite Fermi momentum. Otherwise, in the BEC side, the tightly bound excitons might be formed and they act as a diluted neutral gas. In this situation, the Fermi surface plays no role [41]. In Fig. 2, we present the optical conductivity $\sigma(\omega)$ for different phonon
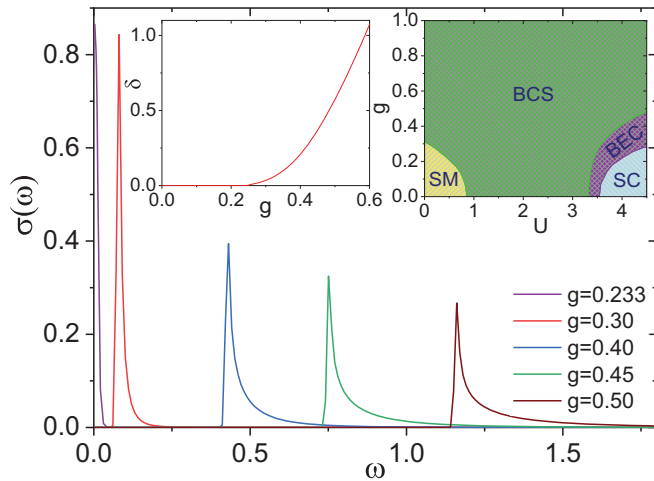
FIG. 3. The optical conductivity $\sigma(\omega)$ for different electron-phonon couplings g at $U = 0.4$ and $\omega_0 = 0.5$. The left inset shows the excitonic condensate order parameter δ as a function of the electron-phonon coupling g. The right inset displays the ground-state phase diagram of the excitonic condensation state in the (U, g) plane.

FIG. 4. The optical conductivity $\sigma(\omega)$ for different electron-phonon couplings g at $U = 4$ and $\omega_0 = 0.5$. The inset shows the excitonic condensate order parameter δ as a function of the electron-phonon coupling g.

frequencies ω_0 at the strong Coulomb interaction $U = 4.0$ and electron-phonon coupling $g = 0.6$. Note here that without the electron-phonon correlations, the system for that Coulomb interaction is in the normal semiconducting state [41]. For small phonon frequency, i.e., in the adiabatic limitation, the optical conductivity spectrum still raises a sharp peak at frequency $\omega = 2\delta$, indicating a BCS-type excitonic condensation state [see Fig. 2(a)]. Increasing the phonon frequency, the influence of phonons on the electron-hole pair bound state is depressed. That signature can be expressed by shifting the peak position to the left for the lower frequency with rapid suppression of the spectral weight. Enlarging phonon frequency in the antiadiabatic regime ($\omega_0 > t^a$), the asymmetric peak still appears in the optical conductivity spectrum but is blunter with a much lower spectral weight. In this case, the system settles in the BEC-type excitonic condensation state (see the right inset in Fig. 1). Deep inside the antiadiabatic regime, the phonon frequency is far from the Fermi level. The electron-phonon correlations are unable to form the electron-hole bound state and the system stabilizes in the normal semiconducting state, indicated by the unnoticeable signature of the optical conductivity [see Fig. 2(b)].

To discuss the influence of the electron-phonon coupling on the optical signatures in the system, in Fig. 3 we show the optical conductivity $\sigma(\omega)$ for different values of the electron-phonon coupling g in the adiabatic condition, for instance at $\omega_0 = 0.5$ with weak Coulomb interaction, $U = 0.4$. In this case of the Coulomb interaction, hybridization between the electrons in the conduction band and the holes in the valence band is not enough to form the bound state of the electron-hole pairs. However, if the electron-phonon correlations are sufficiently large, the bound state of electron-hole pairs might be established and reinforced. Indeed, in the adiabatic situation with $\omega_0 = 0.5$, the excitonic condensate order parameter δ is nonzero if the electron-phonon coupling is larger than a critical value $g_c = 0.233$. The order parameter then rapidly increases as increasing the electron-phonon interaction (see
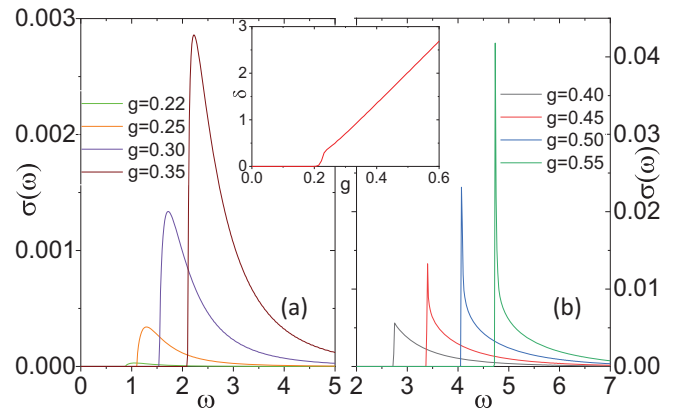
the left inset in Fig. 3). That signature can be probed in the optical conductivity spectra. Actually, for large electron-phonon coupling, one finds the sharp peak in the optical conductivity spectrum at frequency $\omega = 2\delta$ as addressed in Fig. 1. Decreasing the coupling, the sharp peak moves to the left with a lower frequency indicating the depression of the excitonic condensate order parameter. Decreasing the electron-phonon coupling also depresses the possibility of the electrons and holes residing far from the Fermi level coupling together forming the bound state. That is indicated by the acuity of the optical conductivity signature at low g. This acuity signature of the optical conductivity also expresses an important role of the Fermi level in stabilizing the excitonic condensation state or the BCS-type excitonic condensate in the situation. At the critical value of the electron-phonon coupling $g = g_c$, the optical conductivity peaks at zero frequency, indicating the Drude form in the normal semimetal state if $g < g_c$.

On the semiconducting side, i.e., for sufficiently large Coulomb interaction, we also find the interesting signatures of the excitonic excitations by changing the electron-phonon coupling. In Fig. 4, we present the optical conductivity $\sigma(\omega)$ for different values of the electron-phonon coupling g at $\omega_0 = 0.5$ and $U = 4$. At that large Coulomb interaction, the system stabilizes in the normal semiconducting state if there are no electron-phonon correlations [41]. However, by turning on the electron-phonon coupling in the adiabatic situation, the electron-hole coupling might be established and if the electron-phonon coupling is sufficiently strong, the system stabilizes in the excitonic condensation state. Indeed, the inset in Fig. 4 shows that the excitonic condensate order parameter is nonzero only if $g > g_c$. Stabilization of the excitonic condensation state for $g > g_c$ is also addressed by the asymmetric single peak appearance in the optical conductivity spectrum. Indeed, for $g_c < g < 0.4$, Fig. 4(a) shows us the blunter single peak at low frequency in the optical conductivity. That signature is similar to the optical conductivity behavior found in the case of large phonon energy mentioned in Fig. 3(b), indicating the BEC-type condensate of the electron-hole pairs due to the electron-phonon correlations. However, in the case of $g > 0.4$, the single asymmetric peak still appears in the

optical conductivity spectra, but their peak becomes much sharper with higher spectral weight [see Fig. 4(b)]. For this large electron-phonon coupling, the hybridization between electrons in the conduction band and holes in the valance band becomes extremely strong around the Fermi level. The predominance of electrons and holes residing close to the Fermi level coupling together to form the excitonic coherence exhibits the BCS-type excitonic condensation state.

As discussed above, inspecting the optical conductivity spectra gives us the optical absorption properties only for excitons in the condensation state. Investigating excitation of the excitons outside the condensate is thus an essential task to view the excitonic dynamics in a compact picture. In the rest of this paper, we concentrate on addressing the dynamical excitonic susceptibility function to understand the dynamical properties of the exciton system before the condensation state takes place. In the case of Ta_2NiSe_5, one has released the predominance of zero-momentum excitons condensing in a single coherent state [11,16,17]. To be comparable to the experiments, we consider here the dynamical excitonic susceptibility function at the zero momentum $\chi(\omega) \equiv \chi(\mathbf{q} = 0, \omega)$. Figure 5 addresses the imaginary part of the dynamical excitonic susceptibility function $Im\chi(\omega)$ as a function of frequency for different phonon frequencies ω_0 at $g = 0.6$ and for two typical values of Coulomb interaction [$U = 0.4$, Fig. 5(a)] and [$U = 4$, Fig. 5(b)]. Note here that the set of parameters has been chosen as long as the system settles out of the ordered state. For that large electron-phonon coupling, the phonon frequencies must be far from the Fermi level, i.e., in the antiadiabatic regime with $\omega_0 \geqslant 4$ (see the left inset in Fig. 1). Without phonon effects, at small Coulomb interaction, the system settles in the semimetal state and one finds a wide spreading of the dynamical susceptibility with low spectral weight [see the dashed line in Fig. 5(a)]. Tuning the electron-phonon coupling into the system, a peak at low frequency appears and develops as lowering the phonon frequency. The low-energy peak appearance in the dynamical susceptibility function more or less indicates the resonance of the preformed excitonic coherent bound state. Lowering the phonon frequency reinforces the electron-hole pair coherence corresponding to sharpening and moving the peak to the left. That signature of the dynamical excitonic susceptibility function indicates that the bound electron-hole pairs possibly appear in the normal–semimetal state due to the sufficiently large electron-phonon correlations. This theoretical result consolidates recent observations of the preformed excitons appearing before the excitonic condensation state in semimetal Ta_2NiSe_5 [22,23]. Note here that the susceptibility function at high frequency seems to be insignificantly affected by the phonon presence in the system.

In the case of large Coulomb interaction, $U = 4.0$ for instance, the system settles in the semiconducting state (see the right inset in Fig. 1). The imaginary part of the dynamical excitonic susceptibility function expresses a sharp resonance peak at low frequency. The spectral weight here is much larger than that found in the case of the semimetal side [comparing to Fig. 5(a)]. The sharp peak at low frequency here represents the preformed bound electron-hole pair state above the critical point of the semiconducting-excitonic condensate transition. That so-called halo phase has been addressed in the previous
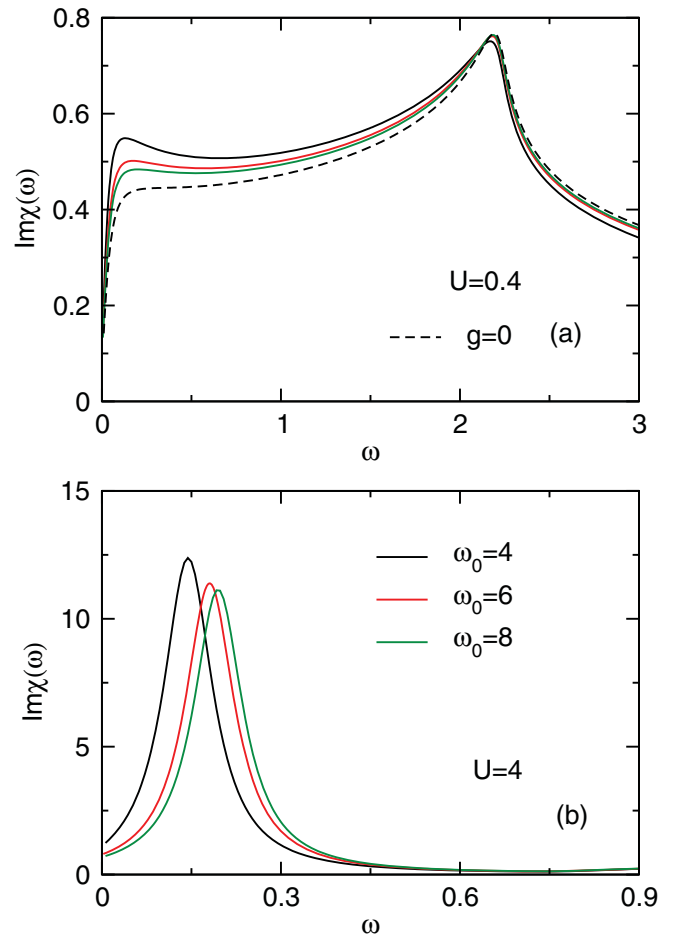
FIG. 5. The imaginary part of the dynamical excitonic susceptibility function as a function of frequency for different values of the phonon frequency ω_0 at $g = 0.6$ with $U = 0.4$ (a) and $U = 4.0$ (b). The dashed line indicates the imaginary part of the dynamical excitonic susceptibility function at $U = 0.4$ and zero electron-phonon coupling $g = 0$.

studies in the EFKM [21]. Taking into account the phonon contributions to the EFKM, one finds a bit of enhancement and shift to the lower energy of the resonance peak. The signature indicates a reinforcement of the electron-hole bound pairs and the halo phase thus is expanded by increasing the electron-phonon correlations.

Lastly, to view in a compact picture the impact of electron-phonon correlations to the excitonic excitations in the system, we discuss signatures of the electron-phonon interaction to the dynamical excitonic susceptibility spectrum. In Fig. 6, we show the imaginary part of the dynamical excitonic susceptibility function $Im\chi(\omega)$ for different values of the electron-phonon coupling g at phonon energy $\omega_0 = 0.5$, i.e., in the adiabatic situation. Both in the semimetal [Fig. 6(a)] and in the semiconducting [Fig. 6(b)] sides, one always finds a small energy peak rising in the dynamical susceptibility spectrum while the electron-phonon coupling is turned on (the high-energy spectrum of the susceptibility function is unchanged). Increasing the electron-phonon interaction, the spectral peak enlarges and shifts to the left with a lower frequency. That signature indicates the bound excitons

FIG. 6. The frequency dependence of the imaginary part of the dynamical excitonic susceptibility function for different values of the electron-phonon coupling g at $\omega_0 = 0.5$ with $U = 0.4$ (a) and $U = 4$ (b).

emphasizes the strong impact of phonons on the preformed coherent excitonic bound state in the system both in the normal semiconducting and the semimetal states.

V. CONCLUSION

In summary, by taking into account the electron-phonon coupling to the extended Falicov-Kimball model, we have analyzed the optical conductivity spectrum and the dynamical excitonic susceptibility function in the framework of the unrestricted Hartree-Fock approximation. The effects of phonons on the low-energy excitations of the excitonic bound state in both semimetal and semiconducting materials have been discussed. Our numerical results supply a compact view of the excitonic dynamical properties both inside and outside of the condensation state. Indeed, inside the excitonic condensate, the optical conductivity spectrum appears a sharp peak at a frequency equal to twice the excitonic order parameter indicating the strong hybridization of the electrons and the holes residing close to the Fermi level. The signature probes the BCS-type excitonic condensation state on the semimetal side. In contrast, on the semiconducting side, the peak in the optical conductivity becomes smeared out addressing the BEC-type excitonic condensation state. The optical conductivity completely disappears while the system settles in the normal–semiconducting regime. Out of the ordered state, the excitonic excitations can be investigated by inspecting the dynamical excitonic susceptibility function. Due to the presence of the electron-phonon correlations, we have specified the possibility of preformed excitons residing in the normal–semimetal state. That signature becomes significant in the case of strong electron-phonon correlations, which has not been mentioned theoretically before or even observed experimentally until recently in Ta_2NiSe_5. In the normal-semiconducting situation, the halo phase with the preformed excitons exiting outside of the BEC-excitonic condensation state has been specified. The halo phase becomes more recognizable by raising the electron-phonon correlations. Inspecting more meticulously the low-energy excitonic excitations by taking into account all other quantum fluctuations would be worthwhile of our future studies.

ACKNOWLEDGMENT

possibly established outside of the excitonic order state in the presence of the electron-phonon coupling. Specifically in the case of strong Coulomb interaction, the sharp peak largely shifts to the low frequency for the electron-phonon coupling risen up to $g = 0.25$ [see Fig. 6(b)] releasing the enhancement of the preformed electron-hole pairs or the halo phase in the semiconducting side. Note here that we are considering the system in the adiabatic situation, so only a slight change of the electron-phonon coupling makes a significant reconstruction of the halo state in the system. The result once more

[1] S. A. Moskalenko and D. W. Snoke, *Bose-Einstein Condensation of Excitons and Biexcitons and Coherent Nonlinear Optics with Excitons* (Cambridge University Press, Cambridge, 2000).

[2] N. F. Mott, Philos. Mag. **6**, 287 (1961).

[3] R. Knox, in *Solid State Physics*, edited by F. Seitz and D. Turnbull (Academic, New York, 1963), Suppl. 5, p. 100.

[4] W. Kohn, in *Many Body Physics*, edited by C. de Witt and R. Balian (Gordon & Breach, New York, 1968).

[5] F. X. Bronold and H. Fehske, Phys. Rev. B **74**, 165107 (2006).

[6] D. Ihle, M. Pfafferott, E. Burovski, F. X. Bronold, and H. Fehske, Phys. Rev. B **78**, 193103 (2008).

[7] V.-N. Phan, K. W. Becker, and H. Fehske, Phys. Rev. B **81**, 205117 (2010).

[8] B. Zenker, D. Ihle, F. X. Bronold, and H. Fehske, Phys. Rev. B **85**, 121102(R) (2012).

[9] P. Wachter, Adv. Mater. Phys. Chem. **08**, 120 (2018).

[10] A. Kogar, M. S. Rak, S. Vig, A. A. Husain, F. Flicker, Y. I. Joe, L. Venema, G. J. MacDougall, T. C. Chiang, E. Fradkin *et al.*, Science **358**, 1314 (2017).

[11] K. Kim, H. Kim, J. Kim, C. Kwon, J. S. Kim, and B. J. Kim, Nat. Commun. **12**, 1969 (2021).

[12] P. Wachter, B. Bucher, and J. Malar, Phys. Rev. B **69**, 094502 (2004).

[13] H. Cercellier, C. Monney, F. Clerc, C. Battaglia, L. Despont, M. G. Garnier, H. Beck, P. Aebi, L. Patthey, H. Berger, and L. Forró, Phys. Rev. Lett. **99**, 146403 (2007).

[14] B. Zenker, H. Fehske, H. Beck, C. Monney, and A. R. Bishop, Phys. Rev. B **88**, 075138 (2013).

[15] Y. Lu, H. Kono, T. Larkin, A. Rost, T. Takayama, A. Boris, B. Keimer, and H. Takagi, Nat. Commun. **8**, 14408 (2017).

[16] P. A. Volkov, M. Ye, H. Lohani, I. Feldman, A. Kanigel, and G. Blumberg, npj Quantum Mater. **6**, 52 (2021).

[17] Y.-S. Zhang, J. A. N. Bruin, Y. Matsumoto, M. Isobe, and H. Takagi, Phys. Rev. B **104**, L121201 (2021).

[18] H. Watanabe, K. Seki, and S. Yunoki, Phys. Rev. B **91**, 205135 (2015).

[19] T.-H.-H. Do, D.-H. Bui, and V.-N. Phan, Europhys. Lett. **119**, 47003 (2017).

[20] T.-H.-H. Do, H.-N. Nguyen, and V.-N. Phan, J. Electron. Mater. **48**, 2677 (2019).

[21] N. V. Phan, H. Fehske, and K. W. Becker, Europhys. Lett. **95**, 17006 (2011).

[22] K. Sugimoto, S. Nishimoto, T. Kaneko, and Y. Ohta, Phys. Rev. Lett. **120**, 247602 (2018).

[23] J. Lee, C.-J. Kang, M. J. Eom, J. S. Kim, B. I. Min, and H. W. Yeom, Phys. Rev. B **99**, 075408 (2019).

[24] D. Geffroy, J. Kaufmann, A. Hariki, P. Gunacker, A. Hausoel, and J. Kuneš, Phys. Rev. Lett. **122**, 127601 (2019).

[25] A. Niyazi, D. Geffroy, and J. Kuneš, Phys. Rev. B **102**, 085159 (2020).

[26] B. Bucher, P. Steiner, and P. Wachter, Phys. Rev. Lett. **67**, 2717 (1991).

[27] Thi-Hong-Hai Do, M.-T. Tran, and V.-N. Phan, Phys. Rev. B **106**, 035120 (2022).

[28] S. Chakrabarty and Z. Nussinov, Phys. Rev. B **84**, 064124 (2011).

[29] A. Georges, G. Kotliar, W. Krauth, and M. J. Rozenberg, Rev. Mod. Phys. **68**, 13 (1996).

[30] U. Gupta and A. K. Rajagopal, Phys. Rev. A **21**, 2064 (1980).

[31] S. Hong and G. D. Mahan, Phys. Rev. B **50**, 7284 (1994).

[32] G. Czycholl, Phys. Rev. B **59**, 2642 (1999).

[33] P. Farkašovský, Phys. Rev. B **77**, 155130 (2008).

[34] C. Schneider and G. Czycholl, Eur. Phys. J. B **64**, 43 (2008).

[35] E. Jeckelmann, F. Gebhard, and F. H. L. Essler, Phys. Rev. Lett. **85**, 3910 (2000).

[36] G. D. Mahan, *Many-Particle Physics* (Kluwer Academic/Plenum Publishers, New York, 2000).

[37] B. Zenker, D. Ihle, F. X. Bronold, and H. Fehske, Phys. Rev. B **81**, 115122 (2010).

[38] H. Bruus and K. Flensberg, *Many-Body Quantum Theory in Condensed Matter Physics: An Introduction* (Oxford University Press, New York, 2004).

[39] A. Nakano, T. Hasegawa, S. Tamura, N. Katayama, S. Tsutsui, and H. Sawa, Phys. Rev. B **98**, 045139 (2018).

[40] M.-J. Kim, A. Schulz, T. Takayama, M. Isobe, H. Takagi, and S. Kaiser, Phys. Rev. Res. **2**, 042039(R) (2020).

[41] T.-H.-H. Do and V.-N. Phan, J. Phys.: Condens. Matter **34**, 165602 (2022).